Supporting Information (SI).

Enhancing Multi-Enzymatic CO_2 Conversion via Reactor Engineering: Effects of Mass Transfer on Sustainable and Green Metrics

Sady Roberto Rodriguez, Marina Guillén & Oscar Romero.*

Bioprocess Engineering and Applied Biocatalysis Group, Department of Chemical, Biological and Environmental Engineering, Universitat Autònoma de Barcelona, 08193 Bellaterra, Spain.

Number of pages: **14**

Figures: **6**

Table: **2**

EXPERIMENTAL

S1. GlyDH and FDH co-immobilization

The co-immobilization of GlyDH and FDH was optimized in earlier work by the authors. (1) Co-immobilization was performed sequentially using crude cell lysates, with a carrier-to-volume ratio of 1:10 on Ni^{2+}-ReliZyme carrier*. A solution with the glycerol dehydrogenase (GlyDH) enzyme was prepared in phosphate buffer 100 mM + NaCl 100 mM (pH 7.5). The enzymatic solution was offered to the carrier and the GlyDH was stabilized by treatment with 0.05% v/v glutaraldehyde at 4 °C for 60 min. The resulting biocatalyst was filtered and washed with immobilization buffer (phosphate buffer 100 mM with NaCl 100 mM, pH 7.5) and two imidazole solutions (20 and 50 mM, with 100 mM NaCl each one). Subsequently, a solution with the formate dehydrogenase enzyme (FDH) [prepared in the same buffer] was offered to the GlyDH immobilized biocatalyst. The final biocatalyst was filtered, washed with immobilization buffer and imidazole 20 mM + NaCl 100 mM, and stored at 4°C. Samples were collected during the process to measure catalytic activity in the blank, suspension, and supernatant of immobilization, as well as protein content according to protocols S2 and S3.

***Carrier preparation:** ReliZyme EP403S carrier was treated with an iminodiacetic acid solution 2 M (pH 11) at a 1:10 support-to-solution ratio and incubated overnight at 25°C. (2) After filtering and washing with water, the resin was functionalized with nickel ions using a nickel sulfate solution 200 mM at a 1:5 support-to-solution ratio, incubating for 2 hours at 25°C. The resulting Ni^{2+}-ReliZyme carrier was then filtered, washed with water, and stored at 4°C.

S2. Catalytic activity tests

FDH and GlyDH activities were measured by NAD^+ reduction to NADH, driven by formate oxidation to CO_2 and glycerol oxidation to DHA, respectively. For FDH, phosphate buffer 100 mM (pH 7.5), sodium formate 50 mM, and NAD^+ 1.67 mM was used, while for GlyDH, glycerol 100 mM in phosphate buffer 100 mM (pH 7.0) and NAD^+ 2.5 mM were employed. Reactions were monitored by measuring NADH production at 340 nm using a Cary 50 Bio spectrophotometer at 30 °C. One unit corresponds to 1 μmol of NADH formed per minute. Duplicate assays were performed.

S3. Protein content by Bradford assay

Total protein concentration was determined using the Bradford assay (3) on a SPECTROstar Nano plate reader (BMG LabTech, Germany) at 595 nm. A calibration curve was generated with bovine serum albumin (BSA) standard in the range of 0–1.0 mg mL^{-1}. For the assay, 200 μL of Bradford reagent was mixed with 7 μL of the sample and incubated for 15 minutes. Triplicate assays were performed.

S4. HPLC analysis

Formate, DHA, and glycerol were quantified using an Agilent 1220 Infinity II liquid chromatograph through ion exchange chromatography. For the analysis, an IC-Sep COREGEL 87H3 column was used and sulfuric acid (H_2SO_4) 0.5 mM and acetonitrile (65:35) as mobile phase. The chromatographic conditions were as follows: flow rate of 0.6 mL min^{-1}, 20 μL of sample injected, column temperature of 35 °C, and detection at 210 nm using a UV/visible detector and an RID detector operating at 35 °C. For glycerol carbonate (GC), reverse-phase chromatography was used with a C-18 CORTECS column and H_2SO_4 0.004 N as the mobile phase. The chromatographic conditions were flow rate

of 0.8 mL min^{-1}, 100 µL of injection volume, and detection using an RID at 35 °C. Triplicate assays were performed.

EQUATIONS

S5. Sensor response time:

(Eq. S1)

$$\tau = \frac{1}{|m|}$$

Where:

m = slope of the line obtained by plotting the natural logarithm of the difference between the saturation concentration (C*) and the measured concentration (C_{mes}) versus time.

S.6 CO_2 balance analysis in the reaction system.

To quantify the mass of CO_2 at the inlet, outlet, and that captured within the system, the following equations were applied:

First, the volume of CO_2 per unit time (L h^{-1}) was calculated for the reactor inlet and outlet following the next equation:

$$\text{Volume of CO2 per unit time (L h - 1)} = \frac{\text{Gas flow rate (mln min - 1)} \times \text{CO2 volume percentage (\%)}}{100}$$

(Eq. S2)

Where:

mln = normal milliliters per minute (mass flow adjusted to standard conditions)

Next, the mass of CO_2 (grams) per unit of time (g h^{-1}) was determined using the ideal gas law equation, incorporating the molecular weight:

(Eq. S3)

$$n = \frac{P \times V \times MW}{R \times T}$$

Where:

n = number of moles of CO_2

P = Pressure of CO_2, in this case 1 atm (established by BCP-CO_2 gas analyzer)

V = Volume of CO_2 per unit of time (either at the inlet or outlet) calculated using Equation S2.

MW = Molecular weight of CO_2 (44.01 g mol^{-1})

R = Ideal gas constant (0.08206 L atm mol^{-1} K^{-1})

T = Absolute temperature, in this case 273.15 K (established by BCP-CO_2 gas analyzer)

The total amount in grams of CO_2 that entered the reactor and the amount captured were calculated by estimating the area under the curve of the graph using the simple trapezoidal rule, as shown in the following equation:

$$\int_a^b f(x)\,dx = \frac{(f(x0) + f(x1)) * (b - a)}{2} \quad \text{(Eq. S4)}$$

Where:

$f(x_0)$ = Function value at the initial point of the interval (g CO_2 h^{-1})

$f(x_1)$ = Function value at the final point of the interval (g CO_2 h^{-1})

(b – a) = Interval width, defined as the difference between the final and initial points, in this case, the time elapsed between two consecutive measurements (h).

In the case of CO_2 converted to formate and glycerol carbonate (GC), only the fraction of CO_2 atoms converted into each product was considered. Accordingly, correction factors (CF) based on molecular weights (MW) were calculated as follows:

(Eq. S5)

$$CF = \frac{MW\ CO2\ (g\ mol\ -\ 1)}{MW\ product\ (g\ mol\ -\ 1)}$$

Where:

MW CO_2 = 44.01 g mol^{-1}

MW Formate = 45.01 g mol^{-1}

MW Glycerol carbonate: 118.09 g mol^{-1}

SCHEMES

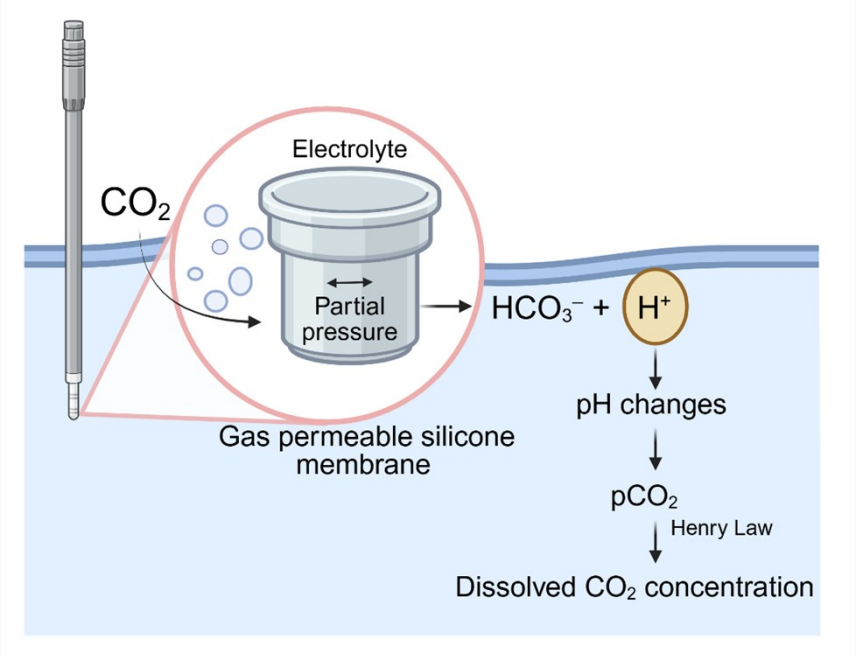

Figure S1. Diagram of the operating principles of the sensor InPro5000*i*/12/220 (Metter Toledo) for measuring dissolved CO_2 in the reaction system.

Brief explanation: The potentiometric measurement of CO_2 using this sensor is based on the Severinghaus principle, a classical method for determining the partial pressure of CO_2 (pCO_2). The sensor consists of a gas-permeable silicone membrane that encloses a specially designed flat pH membrane. Gaseous CO_2 diffuses through the silicone membrane until its partial pressure equilibrates within the pH membrane, which contains

an internal electrolyte solution. The dissolved CO_2 reacts with water to form bicarbonate and H^+ ions:

$$CO_2 + H_2O \leftrightarrow HCO_3^- + H^+$$

The H^+ ions generated induce a pH change in the internal electrolyte, which is detected by the integrated pH electrode. The pCO_2 is then calculated based on the measured pH and temperature. Subsequently, using Henry's law (below), the concentration of dissolved CO_2 in the medium is determined by the sensor.

$$[CO_2] = K_H \cdot pCO_2$$

Where:

K_H = Henry's constant (in mol L^{-1} atm^{-1} or bar^{-1}) which is temperature-dependent.

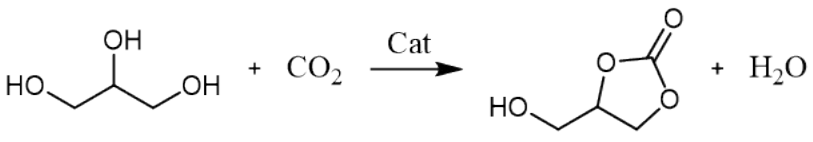

Figure S2. Direct carboxylation reaction between glycerol and CO2 to produce glycerol 1,2-carbonate and water.

RESULTS

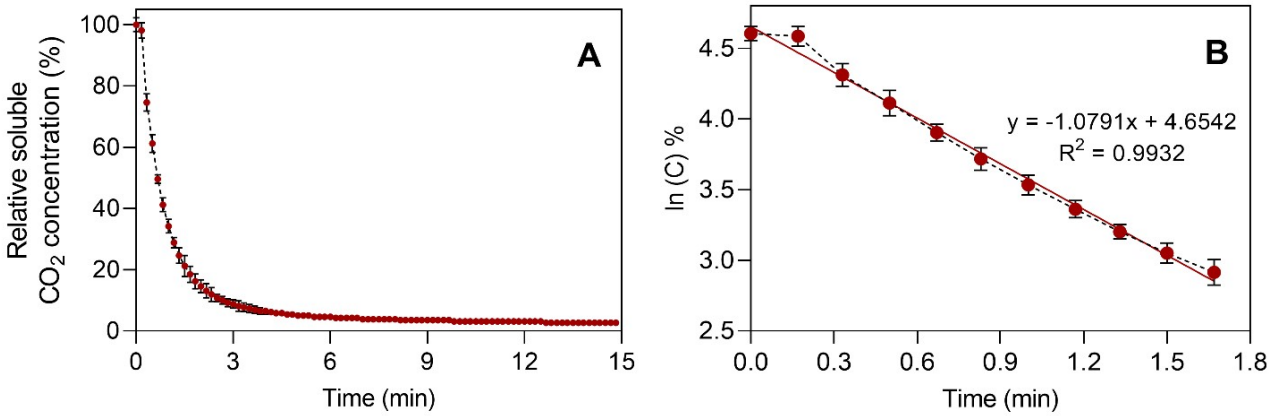

Figure S3. Determination of the response time for the soluble CO_2 sensor. (A) Sensor response over time in a CO_2-free reaction medium. (B) Response time estimation based on the linearized first-order equation.

The response time of this sensor was 0.93 min (56 s), which indicates the time required for the sensor to detect fluctuations in CO_2 concentrations within the medium. This is a tolerable result compared to other CO_2 sensors made from different materials, which exhibit response times ranging from 6 to 164 seconds under similar CO_2 saturation conditions (4–6) , suggesting a reliable sensor operability under these conditions.

Table S1. Determination of the volumetric mass transfer coefficient (k_La) of CO_2 in a stirred-tank reactor by evaluating different volume gas to volume liquid per minute (vvm) from a gas mixture containing 24% CO_2 and the presence of resuspended carrier. (A) Evaluation of different CO_2 sources, (B) Evaluation of different amounts of resuspended Ni^{2+}- ReliZyme and (C) Evaluation of CO_2 source + resuspended Ni^{2+}- ReliZyme.

(A)

CO_2 source	vvm	K_La (min^{-1})	R^2	Gas-Liquid Transfer Rate	
				mg L^{-1} min^{-1} CO_2	mM min^{-1} CO_2
Gas mixture 24% CO_2	0.1	0.01 ± 0.00	0.996	0.36 ± 0.09	0.01 ± 0.00
	0.5	0.09 ± 0.01	0.993	2.95 ± 0.56	0.07 ± 0.01
	1.0	0.16 ± 0.02	0.994	5.55 ± 0.43	0.13 ± 0.01
	1.5	0.17 ± 0.03	0.990	5.85 ± 0.68	0.13 ± 0.02
Pure CO_2	1.0	0.32 ± 0.03	0.990	10.75 ± 0.61	0.24 ± 0.02

(B)

Carrier to total volume (%)	vvm	K_La (min^{-1})	R^2	Gas-Liquid Transfer Rate	
				mg L^{-1} min^{-1} CO_2	mM min^{-1} CO_2
5	1.0	0.21 ± 0.02	0.997	7.17 ± 0.65	0.16 ± 0.01
10		0.22 ± 0.01	0.997	7.35 ± 0.39	0.17 ± 0.01
15		0.16 ± 0.08	0.994	5.55 ± 0.37	0.13 ± 0.01
20		0.12 ± 0.06	0.995	4.03 ± 0.29	0.10 ± 0.00

(C)

CO_2 source + resuspended carrier	vvm	K_La (min^{-1})	R^2	Gas-Liquid Transfer Rate	
				mg L^{-1} min^{-1} CO_2	mM min^{-1} CO_2
Gas mixture 24% CO_2 + 10% Ni^{+2} - ReliZyme	0.1	0.01 ± 0.00	0.990	0.32 ± 0.01	0.01 ± 0.00
	0.5	0.10 ± 0.01	0.999	3.34 ± 0.08	0.08 ± 0.01
	1.0	0.22 ± 0.01	0.997	7.35 ± 0.44	0.17 ± 0.02
	1.5	0.23 ± 0.02	0.997	7.65 ± 0.36	0.17 ± 0.01

Table S2. Performance metrics of the multi-enzymatic reduction of CO_2 to value-added compounds by evaluating different volumetric flow rates (0.5 and 0.1 vvm) using a gas mixture containing 24% CO_2 in a stirred-tank reactor with a 200 mL reaction volume.

Flow volumetric rate (VVM)	Concentration (mM)	STY* (mg L^{-1} h^{-1})	Specific productivity (mg L^{-1} h^{-1} g^{-1} or mg^{-1})		Catalyst yield (mg g^{-1} or mg^{-1})	
			Per catalyst amount (g)	Per total immobilized protein (mg) **	Per catalyst amount(g)	Per total immobilized protein (mg) **
Formate						
1	50.4 ± 0.3	28.4 ± 0.4	1.42 ± 0.09	0.028 ± 0.002	22.7 ± 0.8	0.45 ± 0.08
0.5	57.8 ± 1.1	32.5 ± 1.2	1.63 ± 0.11	0.032 ± 0.001	26.0 ± 1.3	0.52 ± 0.09
0.1	66.1 ± 1.4	37.2 ± 2.2	1.86 ± 0.08	0.037 ± 0.005	29.8 ± 1.7	0.60 ± 0.05
DHA						
1	12.2 ± 0.4	13.7 ± 0.1	0.68 ± 0.04	0.014 ± 0.002	10.9 ± 0.9	0.22 ± 0.09
0.5	8.1 ± 0.3	9.1 ± 0.9	0.46 ± 0.08	0.009 ± 0.001	7.3 ± 0.8	0.15 ± 0.06
0.1	5.2 ± 0.7	5.9 ± 0.6	0.29 ± 0.05	0.006 ± 0.001	4.7 ± 1.4	0.09 ± 0.02
Glycerol carbonate (GC)						
1	40.7 ± 0.2	60.1 ± 2.3	3.00 ± 0.5	--	48.0 ± 2.9	--
0.5	36.9 ± 0.7	54.5 ± 0.4	2.72 ± 0.3	--	43.6 ± 1.2	--
0.1	33.3 ± 1.1	49.1 ± 1.1	2.46 ± 0.4	--	39.3 ± 0.7	--

**STY: Space-time yield. **Total protein amount immobilized on the carrier (CG-GlyDH + FDH*

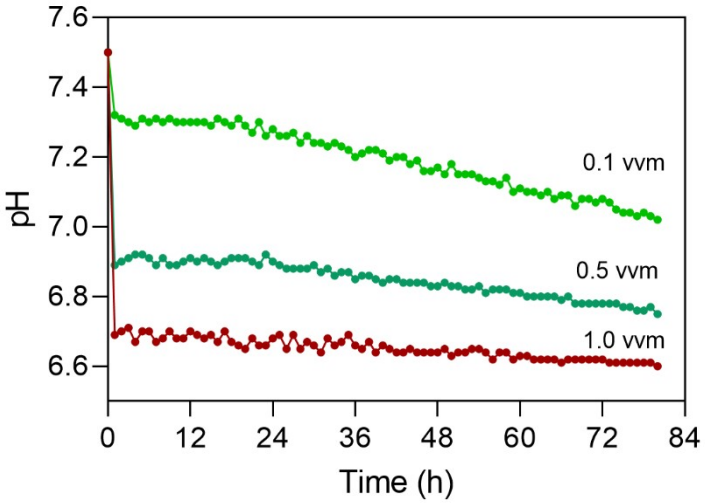

Figure S4. pH monitoring in the multi-enzymatic CO_2 reduction to high-value compounds by evaluating three different gas volumetric flow rates from a 24% CO_2 gas mixture (1.0, 0.5, and 0.1 vvm).

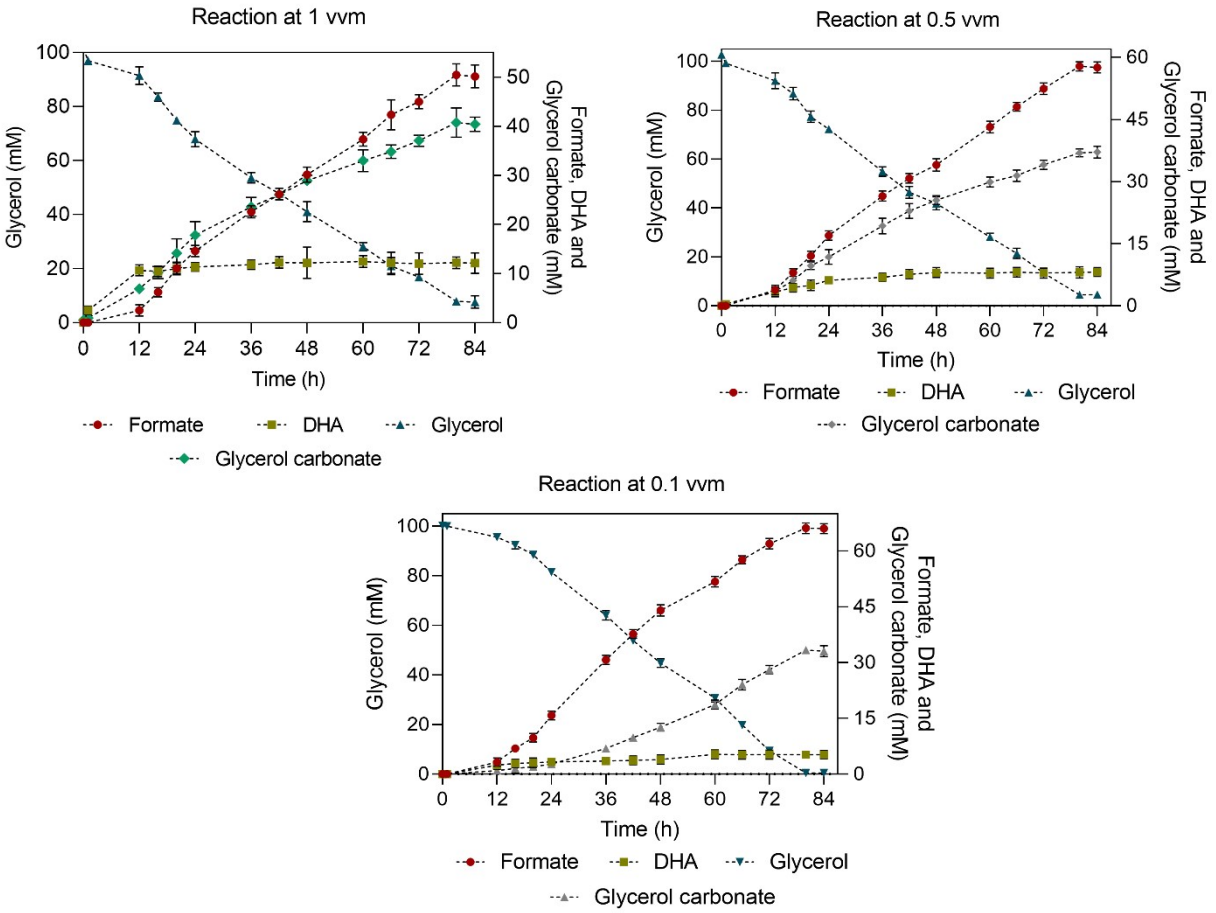

Figure S5. Time course of the multi-enzymatic synthesis of formate and DHA with *in situ* NADH regeneration over 84 hours by evaluating different CO_2 flow rates per reaction volume (1, 0.5 and 0.1 vvm) using a 24% CO_2 gas mixture.

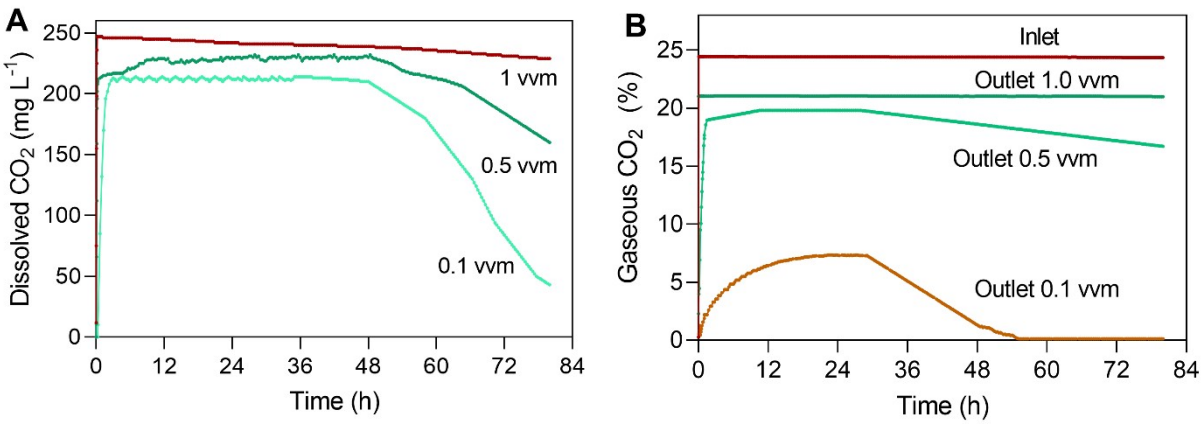

Figure S6. Monitoring dissolved CO_2 concentrations and inlet/outlet CO_2 fractions over 80 hours during the multi-enzymatic reduction of CO_2 by evaluating three different gas volumetric flow

rates (1.0, 0.5, and 0.1 vvm) from a 24% CO_2 gas mixture. (A) Dissolved CO_2 (mg L^{-1}) and (B) CO_2 inlet and outlet fractions (%).

REFERENCES

1. Rodriguez SR, Romero O, Guillén M. Enzyme-Powered CO_2 Utilization: A Bifunctional Immobilized Biocatalyst for Intensified CCU of Industrial Feedstocks to High-Value Chemicals. ACS Sustain Chem Eng. 2026 Jan 12;14(1):86–98. doi:10.1021/acssuschemeng.5c07343

2. Mateo C, Grazu V, Palomo JM, Lopez-Gallego F, Fernandez-Lafuente R, Guisan JM. Immobilization of enzymes on heterofunctional epoxy supports. Nat Protoc. 2007 May 26;2(5):1022–33. doi:10.1038/nprot.2007.133

3. Bradford MM. A Rapid and Sensitive Method for the Quantitation of Microgram Quantities of Protein Utilizing the Principle of Protein-Dye Binding. Anal Biochem. 1976;72(1–2):248–54. doi:10.1016/0003-2697(76)90527-3.

4. González-Garnica M, Galdámez-Martínez A, Malagón F, Ramos CD, Santana G, Abolhassani R, et al. One dimensional Au-ZnO hybrid nanostructures based CO_2 detection: Growth mechanism and role of the seed layer on sensing performance. Sens Actuators B Chem. 2021 Jun 15;337. doi:10.1016/j.snb.2021.129765

5. Kumar V, Singh A, Yadav BC, Singh HK, Singh DP, Singh SK, et al. Environment-sensitive and fast room temperature CO_2 gas sensor based on ZnO, NiO and Ni-ZnO nanocomposite materials. Environ Funct Mater. 2023 Aug;2(2):167–77. doi:10.1016/j.efmat.2023.12.002

6. Amarnath M, Gurunathan K. Highly selective CO_2 gas sensor using stabilized NiO-In_2O_3 nanospheres coated reduced graphene oxide sensing electrodes at room temperature. J Alloys Compd. 2021 Mar 15;857. doi:10.1016/j.jallcom.2020.157584